Progress In Electromagnetics Research, PIER 95, 87–102, 2009

TIME DOMAIN PHYSICAL OPTICS FOR THE HIGHER-ORDER FDTD MODELING IN ELECTROMAGNETIC SCATTERING FROM 3-D COMPLEX AND COMBINED MULTIPLE MATERIALS OBJECTS

F. Faghihi and H. Heydari

Center of Excellence for Power System Automation and Operation
Electrical Engineering Department
Iran University of Science and Technology
Tehran, Iran

Abstract—This paper proposes a hybrid methodology that combines an extended form of Finite-Deference Time-Domain (FDTD) method with Time Domain Physical Optics (TDPO) for analysis of 3-D scattering of combinative objects in complex electromagnetic compatibility (EMC) problems. Establishing a covariant formulation for FDTD, the extended algorithm introduces a parametric topology of accurate nonstandard schemes for the non-orthogonal div-curl problem and the suppression of lattice dispersion. For complex-combined objects including a small size (SS) and large size (LS) parts, using TDPO is an appropriate approach for coupling between two regions. Thus, our technique solves the EMC complexity with the help of higher order FDTD (HOFDTD) and the combinatory structures by using the TDPO. Numerical validation confirms the superiority of the proposed algorithm via realistic EMC applications.

1. INTRODUCTION

The accurate and efficient evaluation of the scattering from a large and complex object is of great interest in engineering [1–4]. Among existing numerical techniques, the finite-difference time-domain (FDTD) method has a wide applicability in many areas of research [5]. Higher order (HO) 3-D FDTD methodology to be a powerful numerical method for such complex and multiple materials structures simulation [6–9]. Furthermore, the development

Corresponding author: H. Heydari (heydari@iust.ac.ir).

of high power microwave antenna, aviation and space techniques has motivated the interest in electromagnetic scattering problems involving combinative objects [10, 20]. The combinative objects are composed by two parts: One is a Small-Size (SS) configuration and the other is a Large-Size (LS) component with respect to the wavelength of interest, such as line surface formation objects, a reflector antenna and a satellite with large wingspan. Generally, neither rigorous numerical method nor asymptotic scheme is easily be implemented in evaluating the time domain scattering for combinative objects exactly and efficiently.

So the hybrid method combining numerical technique with asymptotic approach is invoked in dealing with this class of problems. For complex-combined objects including a SS and LS parts, using Time Domain Physical Optics (TDPO) [21, 22] is suitable technique for coupling between two regions. This paper develops a numerical method that combines higher order FDTD (HOFDTD) with TDPO for the scattering problem by Complex and combinative objects, in which the coupling must be considered by any means. The extended FDTD and TDPO are taken to treat the SS structure and LS part, separately. As the approach is performed in the time domain, it is expected to be appropriate for broad band analysis.

In the following section, we introduce the HOFDTD algorithm to solve complex structure in EMC issues. In Section 3, novel hybrid numerical method that is a combination of HOFDTD with TDPO for electromagnetic scattering from 3-D complex and combined multiple materials objects is explained. In Section 4, two numerical examples which refer to fundamental problems in EMC applications are given to demonstrate the validity of the proposed method and a comparison is made with the results of far field to near field transformation obtained in a previous research.

2. PRELIMINARY ASPECTS: THE GENERALIZED HOFDTD ALGORITHM

When objects of arbitrary curvature and combined materials (multi-materials) are to be modeled, the FDTD technique exhibits an ill-suited behavior, mainly, due to the incomplete imposition of continuity conditions at the interfaces [7, 23]. Unluckily, to these errors one must add the lattice dispersion discrepancies intrinsic in the low-order schemes. A feasible clarification could be the averaging of constitutive parameters at the interfaces [7].

The essential premise of the HO algorithm resides in the representation of electromagnetic fields via a new class of 3-D non-

standard concepts [23–25]. Their form is given by [5, 23]

$$W^{M}_{q,L}[f|^{t}_{u,v,w}] = \frac{g(u,v,w)}{C_S(kL\delta q)} \sum_{m=1}^{M} R^{q}_{m} \times \left\{ \sum_{l=1}^{L} P^{q}_{m,l} D^{(m)}_{q,l\delta q}[[f|^{t}_{u,v,w}]] \right\} \quad (1)$$

where M is the order of accuracy and q is a variable of the general coordinate system (u,v,w) described by its respective g metrics. Such a differencing rationale ensures that dispersion error mechanisms, having the potential to spoil the final outcomes, are drastically subdued or even completely eliminated [8]. On the other hand, parameters R^{q}_{m} and $P^{q}_{m,l}$ achieve an inherent robustness both in the handling of geometric details and the right assignment of field quantities to space-time entities by satisfying the following gauges

$$\sum_{l=1}^{L} R^{q}_{m,l} = 1 \qquad \forall m \quad (2)$$

$$\sum_{m=1}^{M} P^{q}_{m} = \frac{1}{2} \quad (3)$$

Factor L defines the number of stencils, $l\delta q$, along each axis, which are needed for the accomplishment of a specific accuracy with a typical value of $L = 3$. The correction function $C_S(kl\delta q)$ ensures the smooth transition from the continuous to the discrete state. Its argument, depending on wave number k, is selected to handle broadband electromagnetic excitations with the non-standard concepts [8]. This is conducted by employing the Fourier transform of the already computed electric or magnetic vectors at predetermined lattice positions [26]. The process does not affect the total overhead, whereas its efficacy increases with the number of prefixed nodes. A possible choice of C_S could be

$$C_S(kl\delta q) = \frac{16}{k^2} \sin\left(\frac{kl\delta q}{3}\right) \cos\left(\frac{kl\delta q}{9}\right) \quad (4)$$

Operators $D^{(m)}_{q,l\delta q}[.]$, in Equation (1), cover all optimal node arrangements — irrespective of cell shape — leading to very coarse grids and mutual cancellation of material discrepancies.

2.1. The Non-orthogonal Dual-Grid Formulation

Let us recall the previously defined coordinate system ($u = i\delta u, v = j\delta v, w = k\delta w$) and divide a given 3-D domain into uniform cells, as in

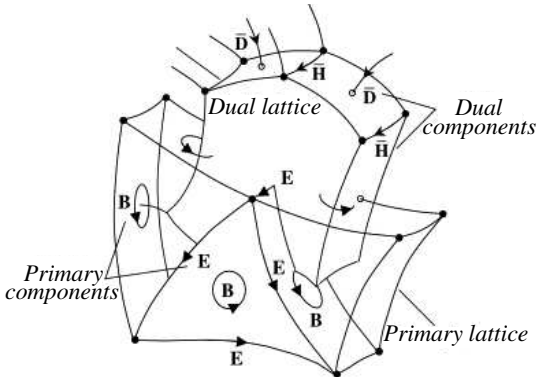

Figure 1. A generalized curvilinear dual FDTD tessellation indicating the positions of electromagnetic intensity and flux field components on the edges and faces of primary and secondary grids. The bar denotes quantities in the secondary lattice [8].

Fig. 1. The center of every primary cell is positioned at (i, j, k), while secondary ones are centered on the vertices of the primary grid [8].

Overall, the HO methodology creates a set of topologically robust forms, which, by constructing a more consistent cell, diminishes late-time instabilities, eliminates dispersion errors and avoids conformal techniques [24–26]. For the termination of infinite problems, we launch a curvilinear non-standard version of the PML, based on an unsplit-field realization. The optimized absorber is built using the proper scaling that retains the original field variation and incorporates the suitable coordinate transformation [23].

2.2. The Convergent Treatment of Arbitrarily-Aligned Material Interfaces

The effects of stair casing on arbitrarily-embedded media interfaces have notable consequences on the convergence of the FDTD method [25]. To defeat this drawback, a HO procedure is expanded that modifies the prior stencils and imposes the suitable continuity situation [27]. Suppose the boundary of Fig. 2, with $\widehat{n} = (\widehat{n}_u, \widehat{n}_v, \widehat{n}_w)^T$ its normal unit vector. The covariant components of E_{cv}^{mt} and H_{cv}^{mt} fields in the two material regions, ε^{mt} and μ^{mt}, for $mt = A, B$, are coupled by [8]

$$\widehat{n} \times E_{cv}^{A} = \widehat{n} \times E_{cv}^{B}, \qquad \varepsilon^{A}\widehat{n}.E_{cv}^{A} = \varepsilon^{B}\widehat{n}.E_{cv}^{B} \tag{5}$$

$$\widehat{n} \times H_{cv}^{A} = \widehat{n} \times H_{cv}^{B}, \qquad \mu^{A}\widehat{n}.H_{cv}^{A} = \mu^{B}\widehat{n}.H_{cv}^{B} \tag{6}$$

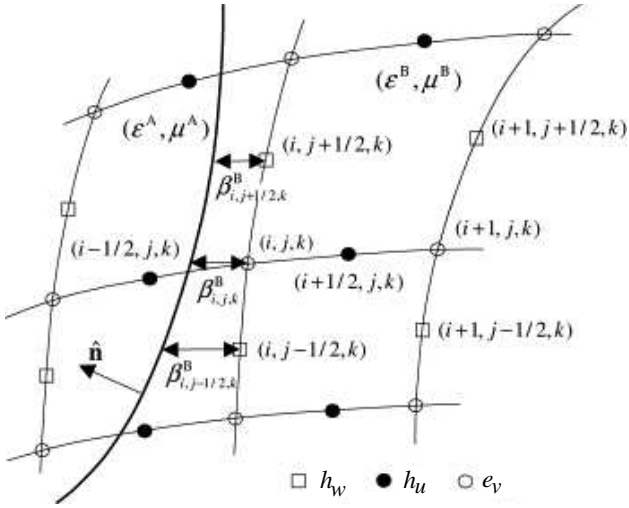

Figure 2. Treatment of a curvilinear arbitrary-aligned material interface, which does not coincide with the grid axes defined by a general coordinate system [23].

Next, we appoint to each region, a parameter, $\beta^{mt}_{i,j,k}$, as an instruction of the distance from the first/last cell to the physical position of the wall relative to cell dimensions [22]. Evidently, $\beta^{mt}_{i,j,k}$ belongs to $[0, 1/2]$ and satisfies $\beta^A_{i,j,k} = 0.5 - \beta^B_{i,j,k}$. Since these coefficients depend only on the boundary's geometrical form, they may be evaluated and stored in a pre-processing step formerly the lattice has been constructed. In this framework [23]:

$$h_u^A \Big|_{i,j,k}^{n+1/2} = \left(1 + \beta^A_{i,j,k}\right) h_u \Big|_{i-1/2,j,k}^{n+1/2} + \beta^A_{i,j,k} h_u \Big|_{i-3/2,j,k}^{n+1/2} \tag{7}$$

is punctually derived. To find h_u, in material B, we first take into account

$$\begin{aligned} 4h_v^A \Big|_{i,j,k}^{n+1/2} &= \widetilde{h}_v \Big|_{i,j-1/2,k-1/2}^{n+1/2} + \widetilde{h}_v \Big|_{i,j+1/2,k-1/2}^{n+1/2} + \widetilde{h}_v \Big|_{i,j+1/2,k+1/2}^{n+1/2} \\ &\quad + \widetilde{h}_v \Big|_{i,j-1/2,k+1/2}^{n+1/2} \end{aligned} \tag{8}$$

$$2h_w^B \Big|_{i,j,k}^{n+1/2} = \widetilde{h}_w \Big|_{i,j+1/2,k}^{n+1/2} + \widetilde{h}_w \Big|_{i,j-1/2,k}^{n+1/2} \tag{9}$$

where the tilde stands for auxiliary magnetic variable evaluated by a simple averaging of the adjacent field values. In this way, the unknown

h_u^B is improved via Equation (7). So:

$$h_u^B\Big|_{i,j,k}^{n+1/2} = h_u^A\Big|_{i,j,k}^{n+1/2} + \widehat{n}_u\left(\mu^A - \mu^B\right) \times \frac{\widehat{n}_u h_u^A\Big|_{i,j,k}^{n+1/2} + \widehat{n}_v h_v^A\Big|_{i,j,k}^{n+1/2} + \widehat{n}_w h_w^B\Big|_{i,j,k}^{n+1/2}}{\mu^A\widehat{n}_w^2 + \mu^B\widehat{n}_u^2 + \mu^B\widehat{n}_v^2} \quad (10)$$

Finally, the nonstandard approximation of $\partial_w h_u$ becomes:

$$LS_w\left[h_u\Big|_{i,j,k}^{n+1/2}\right] = \frac{2\left(2\beta_{i,j,k}^B + 1\right)^{-1}\left(h_u\Big|_{i+1/2,j,k}^{n+1/2} - h_u^B\Big|_{i,j,k}^{n+1/2}\right)}{\Delta u} \quad (11)$$

To apply Equations (7)–(11), a predictor-corrector step is employed where the HOFDTD algorithm, being the predictor, solves Maxwell's equations in the entire domain, while the above technique, performing as the corrector, alters the solutions locally.

3. NOVEL APPROACH FOR ELECTROMAGNETIC SCATTERING OF COMPLEX AND COMBINATIVE MULTIPLE MATERIALS STRUCTURES

Physical optics (PO) is a high frequency approximation technique. The PO phenomena are then used to study the scattering on the ground plane. It is based on an exact formulation of the diffraction problem well known as the Chu-Stratton Equation [21]. Three simplifying assumptions are carried out to decrease the vector integral equation to a simple definite integral over the scatterer surface. It is assumed that:

(a): the surface field over the shadowed portion of the body is *zero*,

(b): the observation point is removed far from the object in term of wavelength and scattering object dimensions,

(c): the dimensions of curvature of the scatterer are large compared to the wavelength.

For a perfectly conducting body, the far scattering field in time-domain is given [21, 22]:

$$\vec{E}(r,t) = (Z_0/4\pi rc) \times \iint_S^{'} \widehat{r} \times \left[\widehat{r} \times \frac{\partial}{\partial t}\vec{J}_S\left(r', t-\tau\right)\right] dS' \quad (12)$$

$$\vec{H}(r,t) = -(1/4\pi rc) \times \iint_S^{'} \widehat{r} \times \frac{\partial}{\partial t}\vec{J}_S\left(r', t-\tau\right) dS' \quad (13)$$

Surface-current density distribution, J_S is written as:

$$\vec{J}_S\left(r',t\right) = \begin{cases} 2\widehat{n'} \times h^{inc}\left(r',t\right) & \text{in the lit region} \\ 0 & \text{otherwise} \end{cases} \tag{14}$$

where h^{inc} is the incident magnetic field. The scattered field can be determined by Equations (12) and (13) if the magnetic field incident on the scatterer is known.

The extended FDTD method has been demonstrated to be an accurate and efficient method to simulate the interaction of electromagnetic waves with all kinds of obstacles, including the target of complex material and complex configuration [23, 24]. Considering the configuration of combinative objects, the computation domain is firstly split into HOFDTD region and TDPO region, enclosing SS and LS structures, respectively. The proposed method uses the two kinds of approach in considering that the total radiated field $e(r,t)$ can be divided into two terms:

$$\vec{e}(r,t) = \vec{e}_i(r,t) + \vec{e}_d(r,t) \tag{15}$$

The first term $e_i(r,t)$, represents the far field directly radiated by the complex element. It can be simply calculated from the HOFDTD algorithm. The second term $e_d(r,t)$ represents the far field scattered by the metallic plane. It can be determined thanks to the TDPO terminology if the magnetic field incident on the scatterer h^{inc}, is known.

In exact expression, the far field can be divided into different terms [21, 22], as follows: The dominant technique of the HOFDTD/TDPO hybrid approach then consists in the interaction between the two regions. First, we consider the influence of HOFDTD region onto TDPO region, as shown in Fig. 3, providing the primary scattered field by SS complex configuration has been obtained by using HOFDTD method.

In order to find the illuminating field onto LS part in TDPO region from SS configuration in HOFDTD region, the near-to-near field extrapolation procedure in HOFDTD is invoked, because HOFDTD region is close to TDPO region. The field illuminated on the surface of LS part can then be defined as:

$$\begin{aligned} h(r,t+\tau) \;=\; \oint_S \Bigg\{ & -\left(\widehat{n}'.\left(\vec{r}-\vec{r}'\right)\right)\left[\frac{h'(r',t)}{4\pi\left|\vec{r}-\vec{r}'\right|^3} + \frac{\frac{\partial h'(r',t)}{\partial t}}{4\pi c\left|\vec{r}-\vec{r}'\right|^2}\right] \\ & - \frac{\frac{\partial h'(r',t)}{\partial n}}{4\pi\left|\vec{r}-\vec{r}'\right|} \Bigg\} ds' \end{aligned} \tag{16}$$

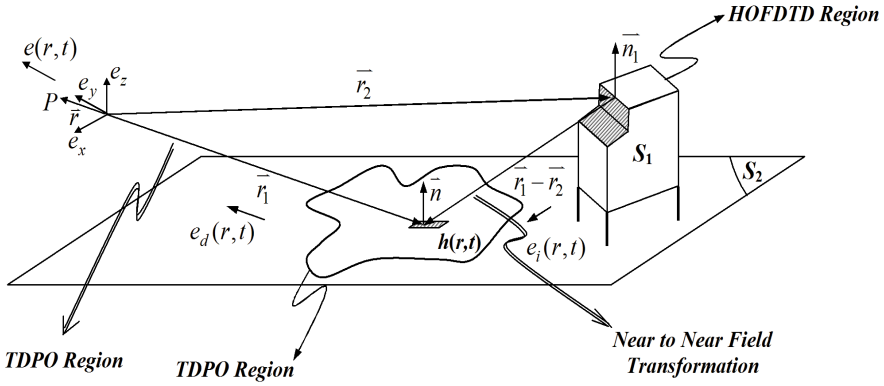

Figure 3. HOFDTD-TDPO hybrid method for field calculation from complex objects.

At time step $n+1$, the time and space derivatives in Equation (16) are approximated by a second-order center difference [28–30]. After several manipulations we may obtain

$$h(r, n+1+\tau/\Delta t) = F_1(n) + F_2(n+1) + F_3(n+2) \qquad (17)$$

where, F_1, F_2 and F_3 are sequences in different time steps [31]. The LS surface in the TDPO area can be divided into M triangular patches, and the recorded time steps in computation are $n\Delta t$ $(n = 1, 2, \ldots, N)$. Due to the incident magnetic field for each time step and allotment point on the surface, the memory storage needs to be a minimum $M \times N^+$, where $N^+ > N$.

Due to retardation from SS to LS part, the continuance of the arrival waveform in the time domain will last much longer than $N\Delta t$. The chronological transfer plan is expanded, so as to decrease the necessity of the computer storage space. In each time step, we execute HOFDTD extrapolation from a cell on HOFDTD output boundary to a patch on the surface of LS part, followed by instantly TDPO calculation of contribution from this patch to the far field surveillance viewpoint.

The substitution of Equation (17) into the Equations (12)–(14) will yield:

$$\vec{E}(r, n+1+(\tau_1+\tau_2)/\Delta t) = \frac{Z_0}{2\pi r c}$$
$$\left(\iint_{S'} \widehat{r} \times \left\{ \widehat{r} \times \left[\widehat{n} \times \widehat{x} \left[\dot{F}_1(n) + \dot{F}_2(n+1) + \dot{F}_3(n+2) \right]_{hx} \right] \right\} dS'$$

$$+\iint_{S'} \widehat{r}\times\left\{\widehat{r}\times\left[\widehat{n}\times\widehat{y}\left[\dot{F}_1(n)+\dot{F}_2(n+1)+\dot{F}_3(n+2)\right]_{hy}\right]\right\}dS'$$
$$+\iint_{S'} \widehat{r}\times\left\{\widehat{r}\times\left[\widehat{n}\times\widehat{z}\left[\dot{F}_1(n)+\dot{F}_2(n+1)+\dot{F}_3(n+2)\right]_{hz}\right]\right\}dS'\Bigg) \quad (18)$$

where, $\dot{F}_i = \partial F_i/\partial t$, $A = Z_0/(2\pi rc)$, and The F terms with different time steps are experientially obtained.

In order to obtain $E(n^*)$ in the observation point, the value at the last time step must be stored. This technique requires a supplementary memory.

We know that E is a sequence in discrete time, where $n^* = int\{n+1+(T_1+T_2)/\Delta t\}$, and at the $(n+1)^{th}$ time step, $F_1(n+1)$, $F_2(n+1)$ and $F_3(n+1)$ are computed, and only $F_2(n+1)$ contributes to $E(n^*)$. $F_1(n+1)$ and $F_3(n+1)$ are added to registers $E(n^*+1)$ and $E(n^*-1)$ in a consistent manner respectively. This approach is used in the proposed algorithm, where the arrows indicate the contribution to E sequence from the FDTD and TDPO iterations.

Now, we present an algorithm of the proposed method as bellow:

1- Applying initial value for the incident field,
2- "A" calculation: Computing the electric and magnetic field from complex objects with HOFDTD,
3- "B" calculation: Computing the electric and magnetic field for LS part with TDPO,
4- "C" calculation: Computing the electric and magnetic field in TDPO region using results of primary scattering field from "A" calculation,
5- "D" calculation: Computing the electric and magnetic field in HOFDTD region using results of primary scattering field from "B" calculation,
6- Final result: Scattered field in observation point for far area is obtained from the primary scattering results ("A" and "B" calculation) and secondary scattering results ("C" and "D" calculation).

This algorithm is performed for each time step.

Based on prior researches [23–25], the stability of the HOFDTD does exist and TDPO has intrinsically stability. As such, the stability of the proposed method can also be taken for granted.

4. NUMERICAL EXAMPLE

In this section two numerical examples which refer to fundamental problems in EMC applications are given to demonstrate the validity

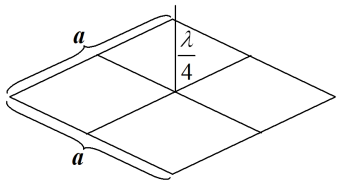

Figure 4. Monopole above finite square ground plane.

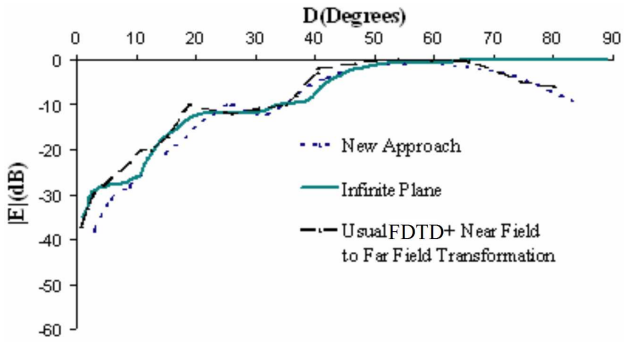

Figure 5. Amplitude pattern for a monopole antenna, the distance $r = 15\,\text{mm}$.

of the proposed method and a comparison is made with the results of near to far field transformation which is presented in [32].

Example 1- To determine the radiation characteristics of a monopole antenna mounted on a large but finite size ground plane has been considered (Fig. 4). The $\lambda/4$ antenna is placed on the center of a plane of dimension $5\lambda \times 5\lambda$ and is excited on their base. The FDTD volume and the ground plane surface are discretized in $\lambda/30$. Furthermore, the radiation characteristics of the same $\lambda/4$ antenna mounted on an infinite plane is performed. It illustrates the effects of the finite scatterer dimensions that are well taken into account by the proposed method for $a = 5\lambda$, $f = 1\,\text{GHz}$.

The results given by the proposed method are compared with the results based on near-field to far-field transformation method [32] and indicate a good agreement which is shown in Fig. 5.

It should be noted that, due to the simplicity of this example the computational speed is similar to the other conventional methods shown in Fig. 5.

Example 2- We consider another practical example of the backscattering by combinative objects composed by a perfect electric

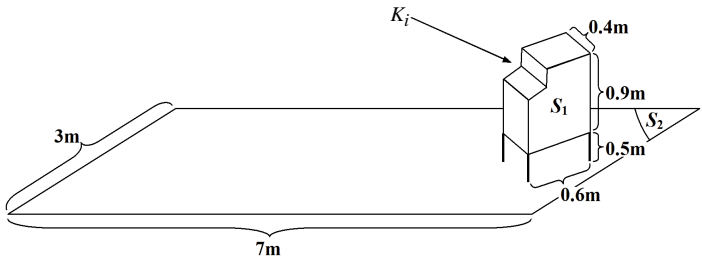

Figure 6. Combinative object composed of complex cube and plate.

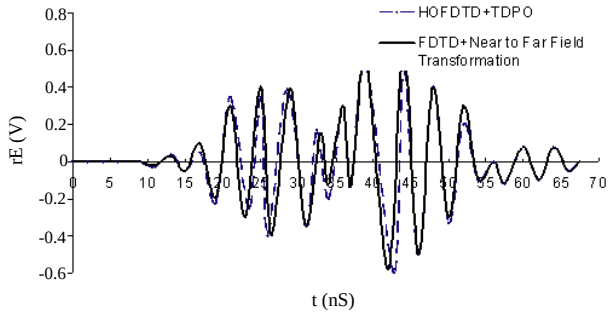

Figure 7. Backscattered waveform in time domain for co-polarization.

conducting (PEC) cube and plate [21, 22], as shown in Fig. 6. A modulated Gaussian pulse with frequency ranging from 200 MHz to 300 MHz, and pulse width 30 ns excites the combinative complex object. The incident wave travels in the xoz plane with $\theta = 45°$ with its electric field parallel to the y-axis. The backscattering for co-polarization is to be established. First, we consider the primary scattering coming from the PEC cube set as an SS structure, and plate as the LS part, respectively. The total scattered field by the studied cube and plate is shown in Fig. 7. The results obtained by the proposed method are compared with the results based on near-field to far-field transformation method [32] and indicates an excellent conformity which is shown in Fig. 7. It is interesting to note that, the accuracy and the speed of computation of the proposed method, (HOFDTD + TDPO), is about 20% and 9% better than FDTD + TDPO method, respectively.

Example 3- Suppose the upper front enclosure in Fig. 6 is made of aluminum material, while the rest of the body is made of iron material,

as shown in Fig. 8. Similar to the Example 2, a modulated Gaussian pulse with frequency ranging from 200 MHz to 300 MHz, and pulse width 30 ns excites the combinative complex object. The incident wave travels in the xoz plane with $\theta = 45^\circ$ with its electric field parallel to the y-axis. The backscattering for co-polarization is to be established. First, we consider the primary scattering coming from the bi-material enclosure set as an SS structure, and plate as the LS part, respectively. The total scattered field by the premeditated enclosure and plate is shown in Fig. 9. It is essential to explain that the results obtain by the proposed algorithm with the help of Equations (5) and (6) for boundary conditions. The results are compared with the results based on near to far field transformation method [32] and indicate an excellent conformity which is shown in Fig. 9. Although, the results differ from the field solution of Case 2 (PEC cube) to some extent, they are in good agreement. The differences in the field are due to the bi-material of the enclosure, in which 2–5% field reduction can be achieved, as compared with PEC.

Furthermore, Fig. 9 will also show that, the speed of computation is very low in the method "FDTD + near to far field transformation" in comparison with the proposed method. On the other hand, the implementation of the conventional method for field solution of the complex configuration with multiple materials (Fig. 8) by ordinary processor can lead to divergence.

As a comparative purpose, suppose there are curve boundaries with two different radius of curvatures with $r = 0.05$ m and $r' = 0.08$ m, as shown in Fig. 10. In this case, for HOFDTD + TDPO there is 35% increase in the speed of field solution, compared with FDTD + TDPO method. However, FDTD + Near to Far Field Transformation the execution time using conventional processor will be very long depending on the field solution methods. There is a $\pm 13\%$ tolerance between FDTD + TDPO and HOFDTD + TDPO methods.

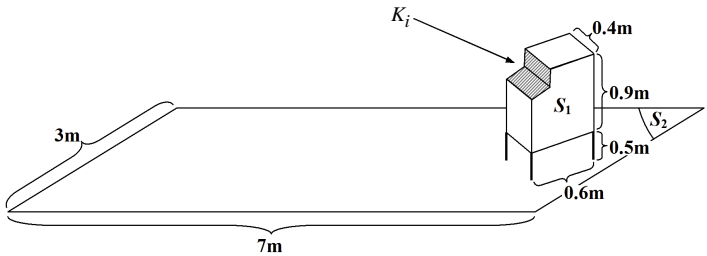

Figure 8. Combinative object composed of bi-material complex enclosure and plate.

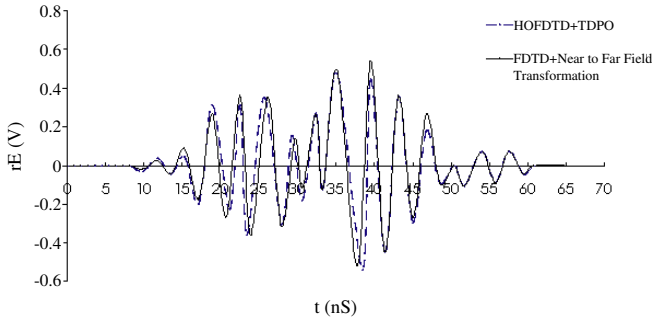

Figure 9. Backscattered waveform in time domain for co-polarization.

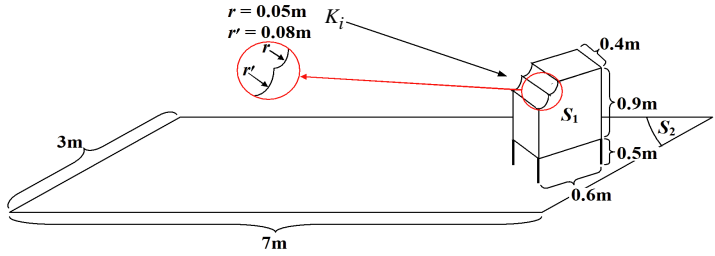

Figure 10.

5. CONCLUSION

A new approach to study small radiation source from complicated configuration close to large scatterer was developed. The approach can be applied to the analysis of the electromagnetic scattering in EMC challenge by complex and combinative multiple materials objects including both SS and LS. The first-order scattering field by LS part in TDPO region is considered as the illuminating field on the LS structure in HOFDTD region, when analyzing the coupling of TDPO to HOFDTD region. The illuminating wave from LS part to SS structure can be introduced through the connection boundary in HOFDTD region. Numerical results for both elementary structure and complex configuration confirm the superiority of the proposed algorithm via realistic Electromagnetic applications. Also, computational comparisons are made with the method based on near-field to far-field transformation and recently proposed method. Specifically, the simulation results for the two different enclosures indicate that the approach can be used for postulate of this paper.

REFERENCES

1. Liu, J. J., "On uniqueness and linearization of an inverse electromagnetic scattering problem," *Applied Mathematics and Computation*, Vol. 171, 406–419, 2005.
2. Rokhlin, V., "Rapid solution of integral equations of scattering theory in two dimensions," *Journal of Computational Physics*, Vol. 86, 414–439, 1990.
3. Liu, J. and J. M. Jin, "A highly effective preconditioner for solving the finite element-boundary integral matrix equation of 3-D scattering," *IEEE Trans. on Antennas and Propagat.*, Vol. 50, 1212–1221, 2002.
4. Liu, J. and J. M. Jin, "A novel hybridization of higher order finite element and boundary integral methods for electromagnetic scattering and radiation problems," *IEEE Trans. on Antennas and Propagat.*, Vol. 49, 1794–1806, 2001.
5. Taflove, A. and S. Hagness, *Computational Electrodynamics: The Finite-difference Time-domain Method*, 2nd edition, Artech House, Boston, 2000.
6. Young, J. L., D. V. Gaitonde, and J. S. Shang, "Toward the construction of a fourth-order difference scheme for transient EM wave simulation: Staggered grid approach," *IEEE Trans. on Antennas and Propagat.*, Vol. 45, 1573–1580, 1997.
7. Kashiwa, T., H. Kudo, Y. Sendo, T. Ohtani, and Y. Kanai, "The phase velocity error and stability condition of three-dimensional nonstandard FDTD method," *IEEE Trans. Magn.*, Vol. 38, 661–664, 2002.
8. Nikolaos, V., N. V. Kantartzis, T. D. Tsiboukis, and E. E. Kriezis, "A topologically consistent class of 3-D higher order curvilinear FDTD schemes for dispersion-optimized EMC and material modeling," *Journal of Materials Processing Technology*, Vol. 161, 210–217, 2005.
9. Wang, M. Y., J. Xu, J. Wu, Y. B. Yan, and H. L. Li, "FDTD study on scattering of metallic column covered by double-negative metamaterial," *Journal of Electromagnetic Waves and Applications*, Vol. 21, No. 14, 1905–1914, 2007.
10. Li, Y.-L., M.-J. Wang, and G.-F. Tang, "The scattering from an elliptic cylinder irradiated by an electromagnetic wave with arbitrary direction and polarization," *Progress In Electromagnetics Research Letters*, Vol. 5, 137–149, 2008.
11. Hillairet, J., J. Sokoloff, and S. Bolioli, "Electromagnetic scattering of a field known on a curved interface using conformal

Gaussian beams," *Progress In Electromagnetics Research B*, Vol. 8, 195–212, 2008.

12. Valagiannopoulos, C. A., "Electromagnetic scattering from two eccentric metamaterial cylinders with frequency-dependent permittivities differing slightly each other," *Progress In Electromagnetics Research B*, Vol. 3, 23–34, 2008.
13. Sun, X. and H. Ha, "Light scattering by large hexagonal column with multiple densely packed inclusions," *Progress In Electromagnetics Research Letters*, Vol. 3, 105–112, 2008.
14. Hamid, A.-K. and F. R. Cooray, "Scattering by a perfect electromagnetic conducting elliptic cylinder," *Progress In Electromagnetics Research Letters*, Vol. 10, 59–67, 2009.
15. Fan, Z., D.-Z. Ding, and R.-S. Chen, "The efficient analysis of electromagnetic scattering from composite structures using hybrid Cfie-Iefie," *Progress In Electromagnetics Research B*, Vol. 10, 131–143, 2008.
16. Hua, Y., Q. Z. Liu, Y. L. Zou, and L. Sun, "A hybrid fe-bi method for electromagnetic scattering from dielectric bodies partially covered by conductors," *Journal of Electromagnetic Waves and Applications*, Vol. 22, No. 2–3, 423–430, 2008.
17. Wang, R. and L. Guo, "Numerical simulations wave scattering from two-layered rough interface," *Progress In Electromagnetics Research B*, Vol. 10, 163–175, 2008.
18. Huang, T., Y. Zhang, L. Li, W. Shao, and S.-J. Lai, "Modified incomplete Cholesky factorization for solving electromagnetic scattering problems," *Progress In Electromagnetics Research B*, Vol. 13, 41–58, 2009.
19. Wang, Y., K. C. Sujeet, and S. N. Safieddin, "An FDTD/raytracing analysis method for wave penetration through inhomogeneous walls," *IEEE Trans. on Antennas and Propagat.*, Vol. 50, 1598–1604, 2002.
20. Nie, X.-C., Y.-B. Gan, N. Yuan, C.-F. Wang, and L.-W. Li, "An efficient hybrid method for analysis of slot arrays enclosed by a large radome," *Journal of Electromagnetic Waves and Applications*, Vol. 20, No. 2, 249–264, 2006.
21. Sun, E.-Y. and W. V. T. Rusch, "Time-domain physical-optics," *IEEE Trans. on Antennas and Propagat.*, Vol. 42, 9–15, 1994.
22. Yang, L.-X., D.-B. Ge, and B. Wei, "FDTD/TDPO hybrid approach for analysis of the EM scattering of combinative objects," *Progress In Electromagnetics Research*, PIER 76, 275–284, 2007.

23. Kantartzis, N. V. and T. D. Tsiboukis, "A higher order nonstandard FDTD-PML method for the advanced modeling of complex EMC problems in generalized 3-D curvilinear coordinates," *IEEE Transaction Electromagnetic Compatibility*, Vol. 46, 2–8, 2004.
24. Zygiridis, T. T. and T. D. Tsiboukis, "Optimized three-dimensional FDTD discretizations of Maxwell's equations on Cartesian grids," *Journal of Computational Physics*, Vol. 226, 2372–2388, 2007.
25. Nikolaos, V. K. and T. D. Tsiboukis, "Rigorous ADI-FDTD analysis of left-handed metamaterials in optimally-designed EMC applications," *COMPEL: The International Journal for Computation and Mathematics in Electrical and Electronic Engineering*, Vol. 25, 667–690, 2006.
26. Petropoulos, P. G., L. P. Zhao, and A. C. Cangellaris, "A reflectionless sponge layer absorbing boundary condition for the solution of Maxwell's equations with high-order staggered finite differences," *Journal of Computational Physics*, Vol. 139, 184–208, 1998.
27. Lee, J.-F., R. Palendech, and R. Mittra, "Modeling three-dimensional discontinuities in waveguides using the non-orthogonal FDTD algorithm," *IEEE Trans. Microwave Theory Tech.*, Vol. 40, 346–352, 1992.
28. Rao, S. M. and D. R. Wilton, "E-field, H-field, and combined field solution for arbitrarily shaped three-dimensional dielectric bodies," *Electromagn.*, Vol. 10, 407–421, 1990.
29. Jiao, D., A. A. Ergin, B. Shanker, E. Michielssen, and J. M. Jin, "A fast higher-order time-domain finite element-boundary integral method for 3-D electromagnetic scattering analysis," *IEEE Trans. on Antennas and Propagat.*, Vol. 50, 1192–1202, 2002.
30. McCowen, A., A. J. Radcliffe, and M. S. Towers, "Time-domain modeling of scattering from arbitrary cylinders in two dimensions using a hybrid finite-element and integral equation method," *IEEE Trans. Magn.*, Vol. 39, 1227–1229, 2003.
31. Ramahi, O. M., "Near- and far-field calculations in FDTD simulations using Kirchhoff surface integral representation," *IEEE Trans. on Antennas and Propagat.*, Vol. 45, 753–759, 1997.
32. Costanzo, S. and G. D. Massa, "Near-field to far-field transformation with planar spiral scanning," *Progress In Electromagnetics Research*, PIER 73, 49–59, 2007.